SAND2022-12977C

DEMSI
Discrete Element Model for Sea Ice

Sandia National Laboratories

Los Alamos NATIONAL LABORATORY EST. 1943

Modeling Arctic Sea Ice with a Discrete Element Model



Kara Peterson, Dan Bolintineanu, Svetoslav Nikolov,
Joel Clemmer, Devin O'Connor
Sandia National Laboratories

Adrian Turner
Los Alamos National Laboratory

Meshfree and Novel Finite Element Methods with Applications (MFEM)
September 26, 2022

SciDAC
Scientific Discovery through Advanced Computing

Sandia National Laboratories is a multimission laboratory managed and operated by National Technology & Engineering Solutions of Sandia, LLC, a wholly owned subsidiary of Honeywell International Inc., for the U.S. Department of Energy's National Nuclear Security Administration under contract DE-NA0003525.

U.S. DEPARTMENT OF ENERGY NNSA

Sandia National Laboratories is a multimission laboratory managed and operated by National Technology and Engineering Solutions of Sandia LLC, a wholly owned subsidiary of Honeywell International Inc. for the U.S. Department of Energy's National Nuclear Security Administration under contract DE-NA0003525.

SANDxxxxx C

SEA ICE IN THE EARTH SYSTEM

Importance in global climate

- Reflects solar radiation
- Insulates ocean from atmosphere
- Influences ocean circulation

Sea ice models must capture

- Mechanical deformation due to surface winds and ocean currents
- Formation of leads (cracks) and pressure ridges
- Annual cycle of growth and melt due to radiative forcing

Visualizations by Trent L. Schindler https://svs.gsfc.nasa.gov/

SEA ICE MODELING

- Most sea ice models in coupled Earth system models use a continuum formulation (Turner et al. 2022, Rampal et al. 2016)
- At high resolutions (~5-6 km) isotropic continuum models do not approximate the dynamics well
- Discrete element method
  - Lagrangian particles
  - Captures anisotropic, heterogenous nature of sea ice deformation
  - Explicit fracture and break-up of pack
- Previous DEM sea ice modeling efforts focused primarily on regional scale, short-term simulations (Hopkins 2004)

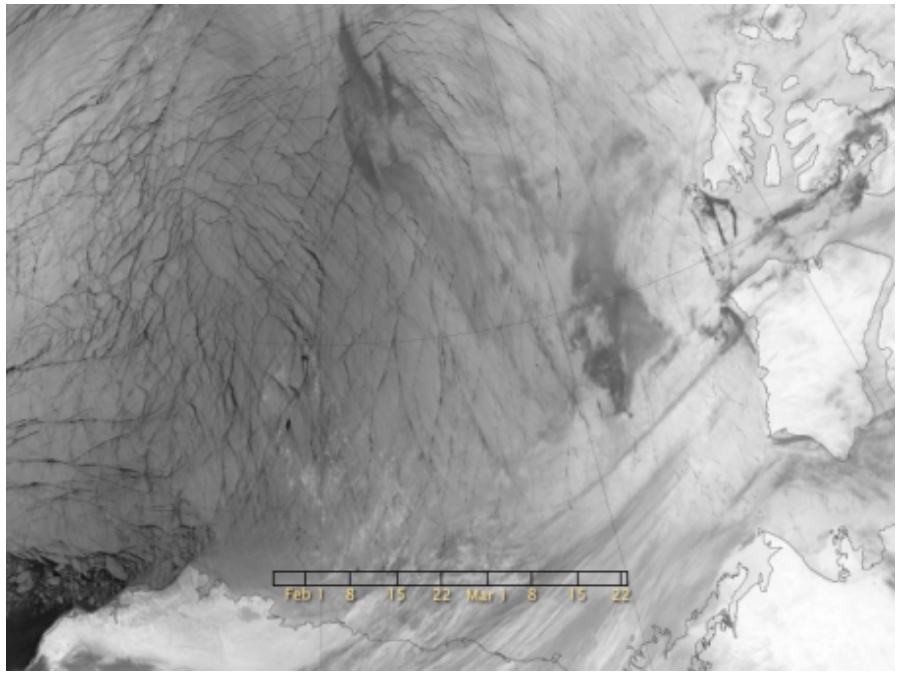

NASA Earth Observatory images by Jesse Allen using VIIRS day -night band data from the Suomi National Polar-orbiting Partnership.
https://visibleearth.nasa.gov/images/80752/extensive-ice-fractures-in-the-beaufort-sea/80756l

Our objective is to develop a computationally efficient global climate scale sea ice model using DEM.

DISCRETE ELEMENT MODEL FOR SEA ICE (DEMSI)

Dynamics: *Large-scale Atomic/Molecular Massively Parallel Simulator (LAMMPS) (Thompson et al. 2022)*

- Particle based molecular dynamics code
- Includes support for DEM and history dependent contact models

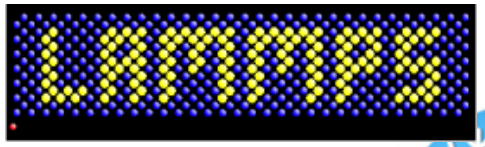

Thermodynamics: *CICE Consortium Icepack Library (Hunke et al. 2018)*

- State-of-the-art sea-ice thermodynamics package
- Includes vertical thermodynamics, salinity, shortwave radiation, snow, melt ponds, ice thickness distribution, biogeochemistry

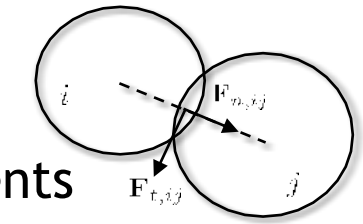

- Dynamics are computed using circular Lagrangian elements
- Interactions via contact forces for bonded and unbonded elements
- Enables capture of complex anisotropic deformation and fracture

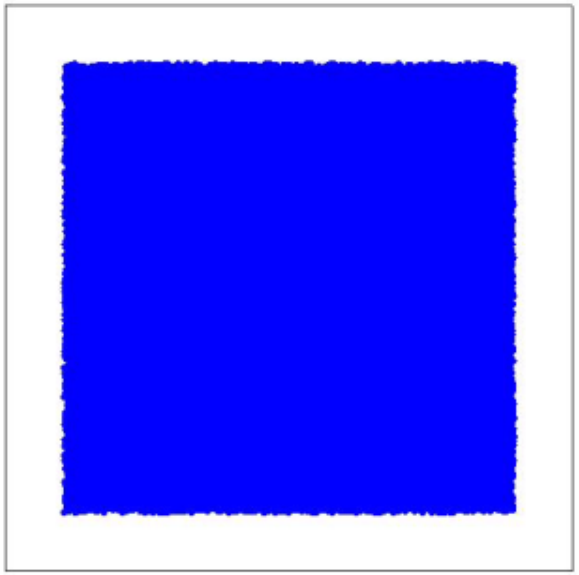

REPRESENTATION OF SEA ICE IN DEMSI

- Individual ice floes are not resolved at the climate modeling scale
- Each circular discrete element particle represents a region of ice with varying thickness including open water
- Sea ice column thermodynamics model (Icepack) evolves
  - Ice thickness distribution
  - Ice concentration or fractional area of ice in each element
  - Ice thermodynamics (temperature/enthalpy) in vertical layers
- Discrete element contact model evolves 2-D sea ice dynamics
  - Velocity convergence/divergence impacts ice thickness distribution
- Effective particle area
  - Defined by Voronoi tessellation of particles
  - Provides a method to define conserved quantities covering the domain

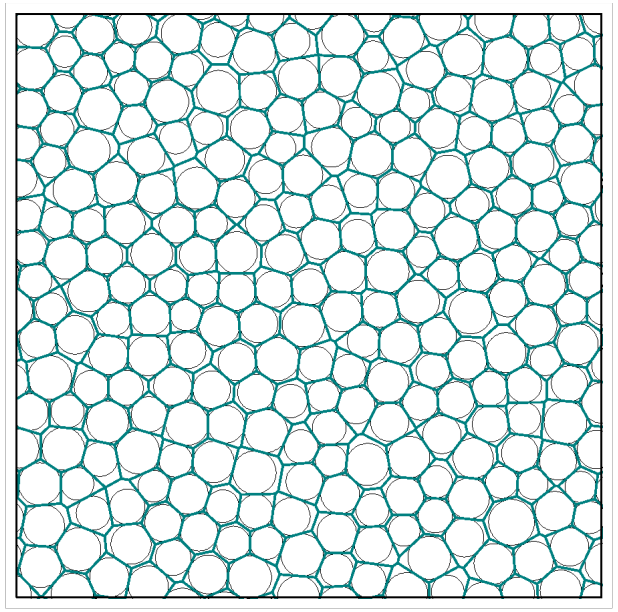

CONTACT MODEL

- Based the work of Hopkins 2004, Wilchinsky et al. 2010 applied to circular elements
- Sets normal ($F\_(n,ij)$) and tangential ($F\_(t,ij)$) forces
- Considers bonded and unbonded states
  - Mechanical forces break up bonds
  - Freezing/solidification creates bonds between elements
- Viscous dampening force added to bonded elements based on Siku model in Kulchitsky et al., 2017
- Includes sea ice ridging under convergence

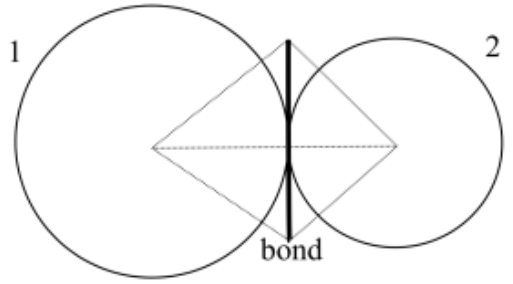

Two particles in equilibrium
($F_{n,ij} = F_{t,ij} = 0$)

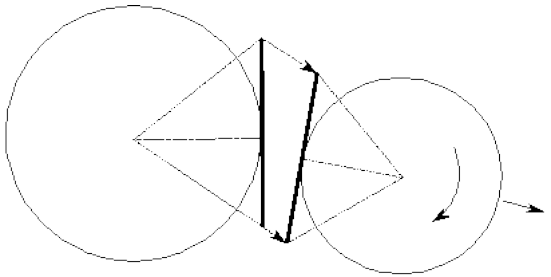

Two bonded particles in relative motion

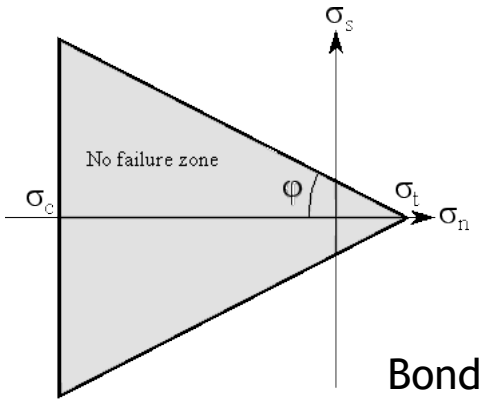

Bond failure set by Mohr-Coulomb fracture law

Total force on particle i: $\mathbf{F}_i = \sum_{j,j\neq i}^{N} (\mathbf{F}_{n,ij} + \mathbf{F}_{t,ij}) + \mathbf{F}_{ext}(\mathbf{r}_i)$

$$\mathbf{F}_{ext}(\mathbf{r}_i) = \rho_a C_a \|\mathbf{v}_a\| \mathbf{v}_a \pi R_i^2 + \rho_w C_w \|\mathbf{v}_w - \mathbf{v}_i\| (\mathbf{v}_w - \mathbf{v}_i) \pi R_i^2 - f_c m_i (\mathbf{k} \times \mathbf{v}_i) + f_c m_i (\mathbf{k} \times \mathbf{v}_w)$$

Wind drag | Ocean drag | Coriolis force | Surface tilt

COMPUTATIONAL PERFORMANCE

- Contact model implemented in LAMMPS
  - Computationally efficient providing high-performance baseline
  - Leverages Kokkos ecosystem for performance portability
- Good strong scaling results for uniform stress test case with varying particle count

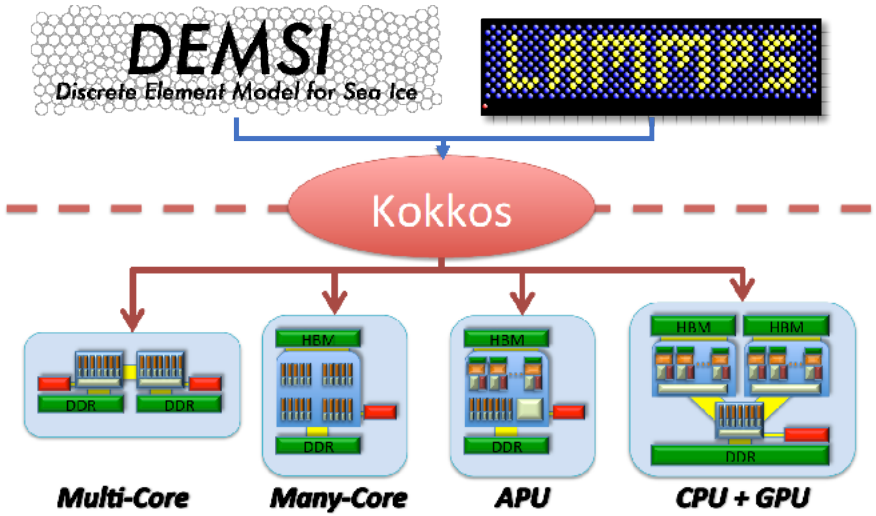

https://github.com/kokkos

Strong scaling on CPU

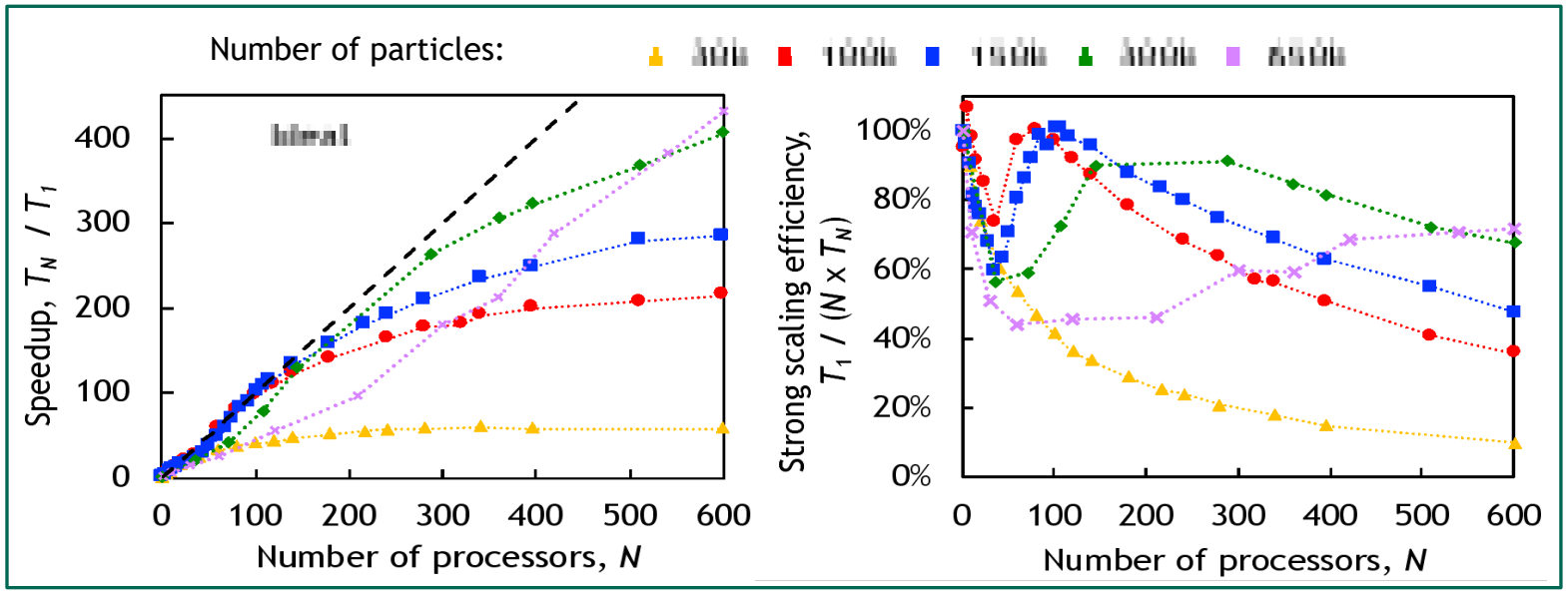

Preliminary look at GPU performance: Results for Nvidia Tesla P100 GPU node versus Power8 node with eight Garrison dual socket cores

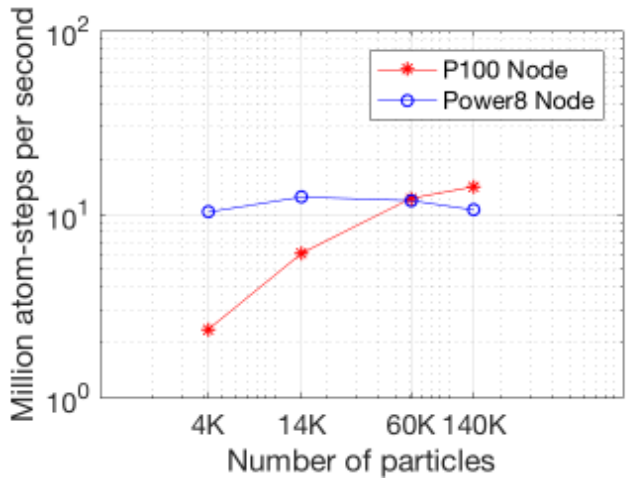

INTERPOLATION & REMAP IN DEMSI

Coupling with ocean and atmosphere models

- DEMSI under development for the Energy Exascale Earth System Model (E3SM)
- Requires interpolation between Lagrangian particles and Eulerian grids
- Work to incorporate unstructured Voronoi grid in DEMSI is ongoing

Particle-to-particle remap

- Periodic remap to initial particle distribution to manage large deformations and particle clustering
- Provides method for adding new particles due to thermodynamic growth

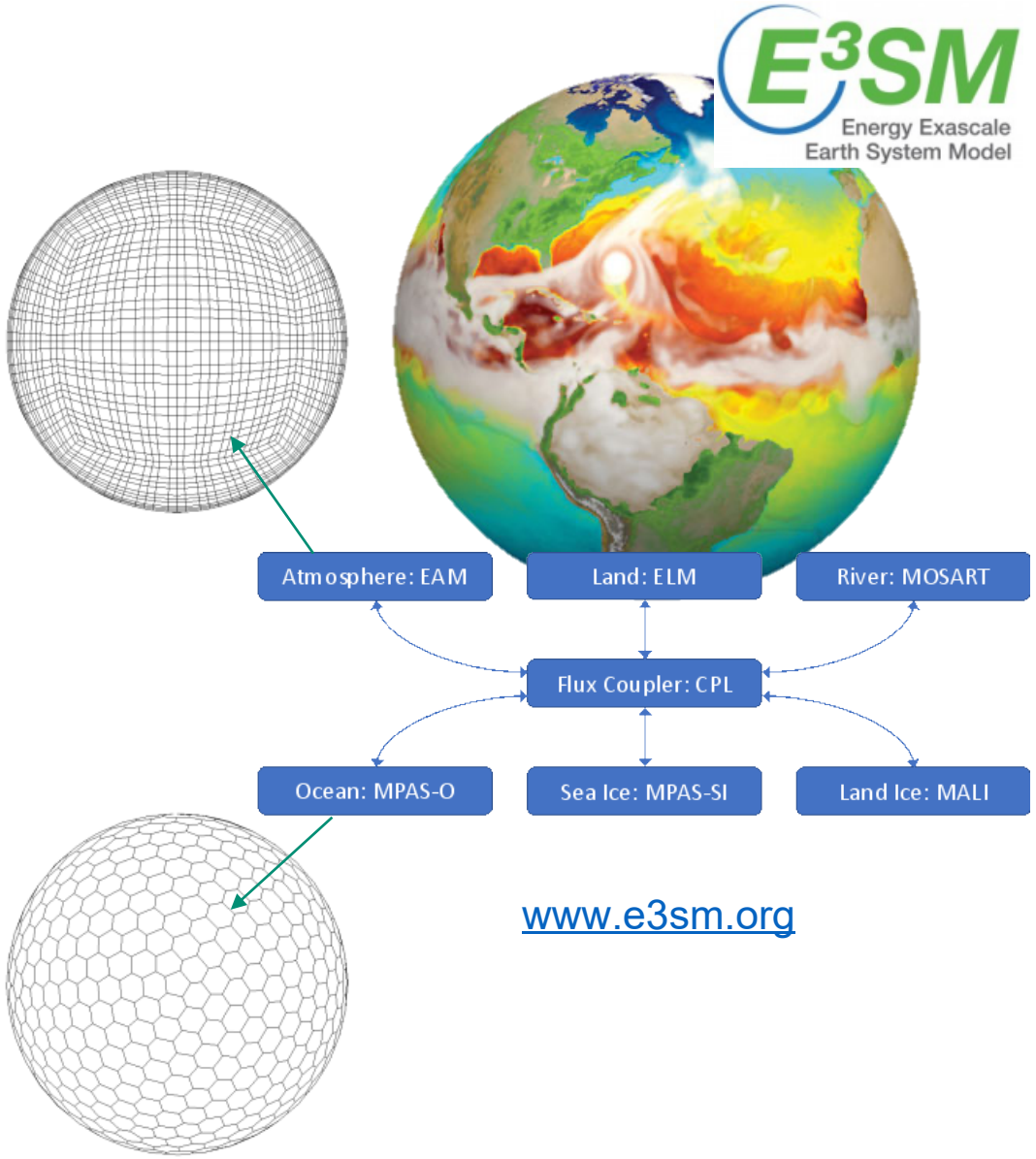

GEOMETRIC REMAP

- Adapted geometric remap algorithm to spherical particles (Turner, *et al*. GMD 2022).
- Conservative, bounds preserving, and 2nd order accurate.
- Compatible remap for hierarchical set of tracers depending on sea ice fractional area and volume.

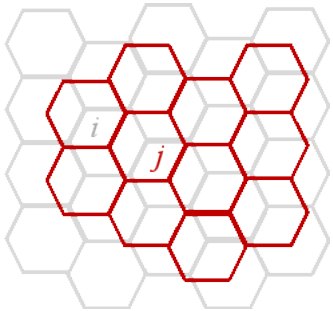

Steps in Algorithm

1. Determine overlap polygons and remap effective element area $$e_j = \sum_i e_{ij} = \sum_i \frac{A_{P_{ij}}}{A_{P_i}} e_i.$$

2. Compute linear reconstructions of average tracer fields $$c^p(\mathbf{r}) = c + \alpha_c \nabla c \cdot (\mathbf{r} - \bar{\mathbf{r}}) \quad \bar{\mathbf{r}} = \frac{1}{A} \int_A \mathbf{r}\, dA,$$

3. Integrate conserved variable reconstructions over intersection polygons $$\mathcal{A}_{jk} = \sum_i e_{ij} \frac{1}{A_{P_{ij}}} \int_{A_{P_{ij}}} c^p_{ik}(\mathbf{r})\, dA,$$

4. Enforce bounds preservation using optimization-based flux correction

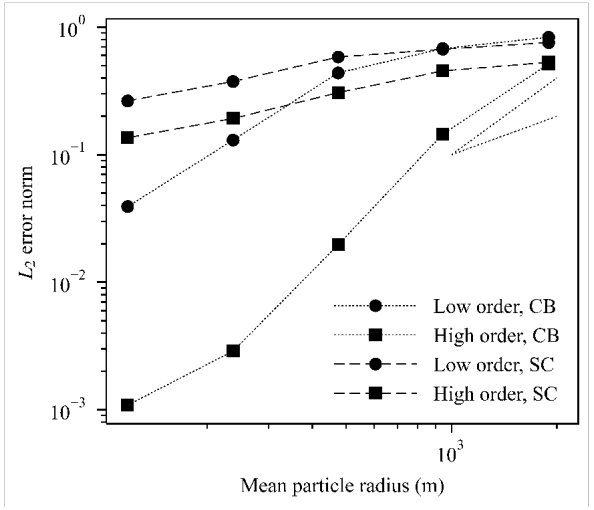

- Cosine bell and slotted cylinder
- Irregular initial particle distribution
- 100 km of translation (200 time steps)

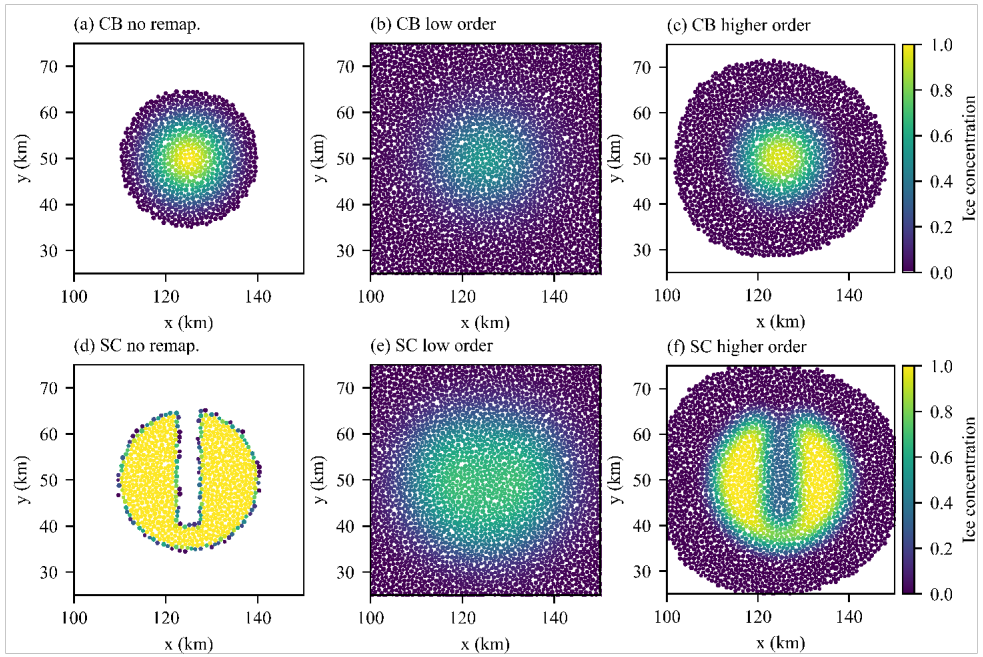

CONTACT MODEL UNIAXIAL COMPRESSION

- Holding all parameters constants except bond moduli (E_b) and bond thickness (h_m).
- Brittle-like failure as E_b and h_m increase.
- Consistent with results in the literature (Herman 2016).
  - E_b = 1 Gpa (when varying h_m)
  - h_m = 0.2 m (when varying E_b)

Contact parameter
Compressive breaking stress coeff. = 1285.0
Tensile breaking stress coeff. = 0.1
Friction angle = 13.0°
Bonded damping coeff. = 1.0 x 10^4
Tangential friction coeff. = 0.3
Nonbonded normal damping coeff. = 0.1
Nonbonded tangential damping coeff. = 1.0 x 10^5
Critical crushing thickness = 0.2 m
Plastic friction coeff. = 26126.0 N/m
Plastic hardening coeff. = 9.28 N/m^2
Poisson ratio = 0.3

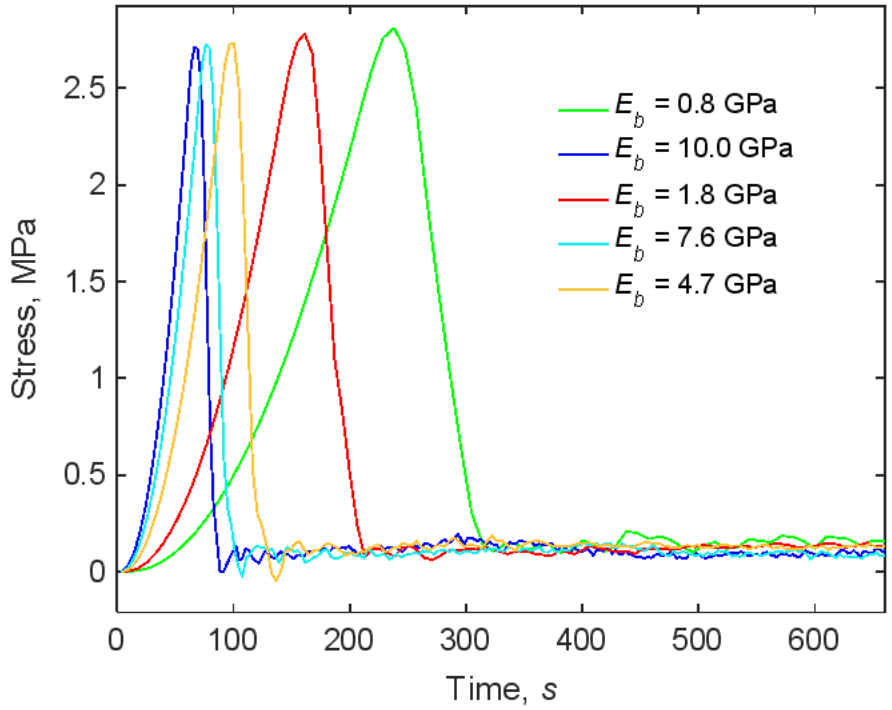

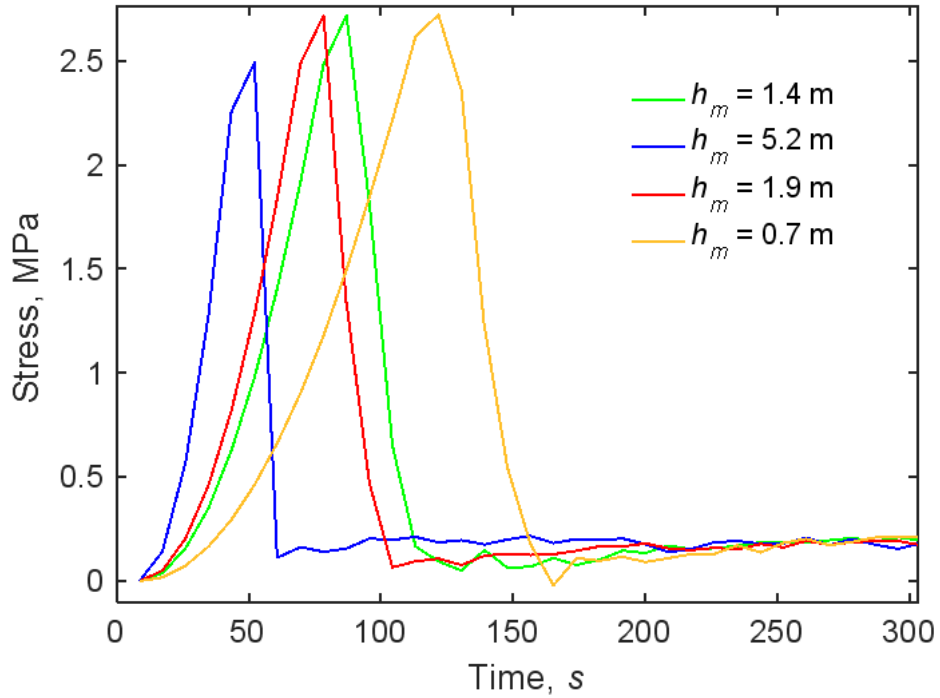

CONTACT MODEL PARAMETER SENSITIVITY ANALYSIS

- Sensitivity analysis is first step in parameter optimization and calibration.
- Mechanical test cases: compression, tension, shear.
- 2 sample test sizes: 2 km x 2.4 km, 3.2 km x 6.4 km.
- 13 contact parameters.
- Sobol sensitivity analysis with Saltelli sampling.

X_i	Contact parameter	Low. bnd.	Upp. bnd.	Unit
1	Compressive breaking stress coeff.	100	5000	-
2	Tensile breaking stress coeff.	0.01	0.9	-
3	Friction angle	12	19	°
4	Bonded damping coeff.	1000	$5x10^4$	-
5	Tangential friction coeff.	0.05	0.7	-
6	Nonbonded normal damping coeff.	0.01	0.7	-
7	Nonbonded tangential damping coeff.	$1x10^4$	$5x10^5$	-
8	Critical crushing thickness	0.01	0.7	m
9	Elastic modulus	$1x10^8$	$1x10^{10}$	Pa
10	Bond thickness	0.1	10	m
11	Plastic friction coeff.	6000	$4.6x10^4$	N/m
12	Plastic hardening coeff.	5	15	N/m^2
13	Poisson ratio	0.2	0.45	-

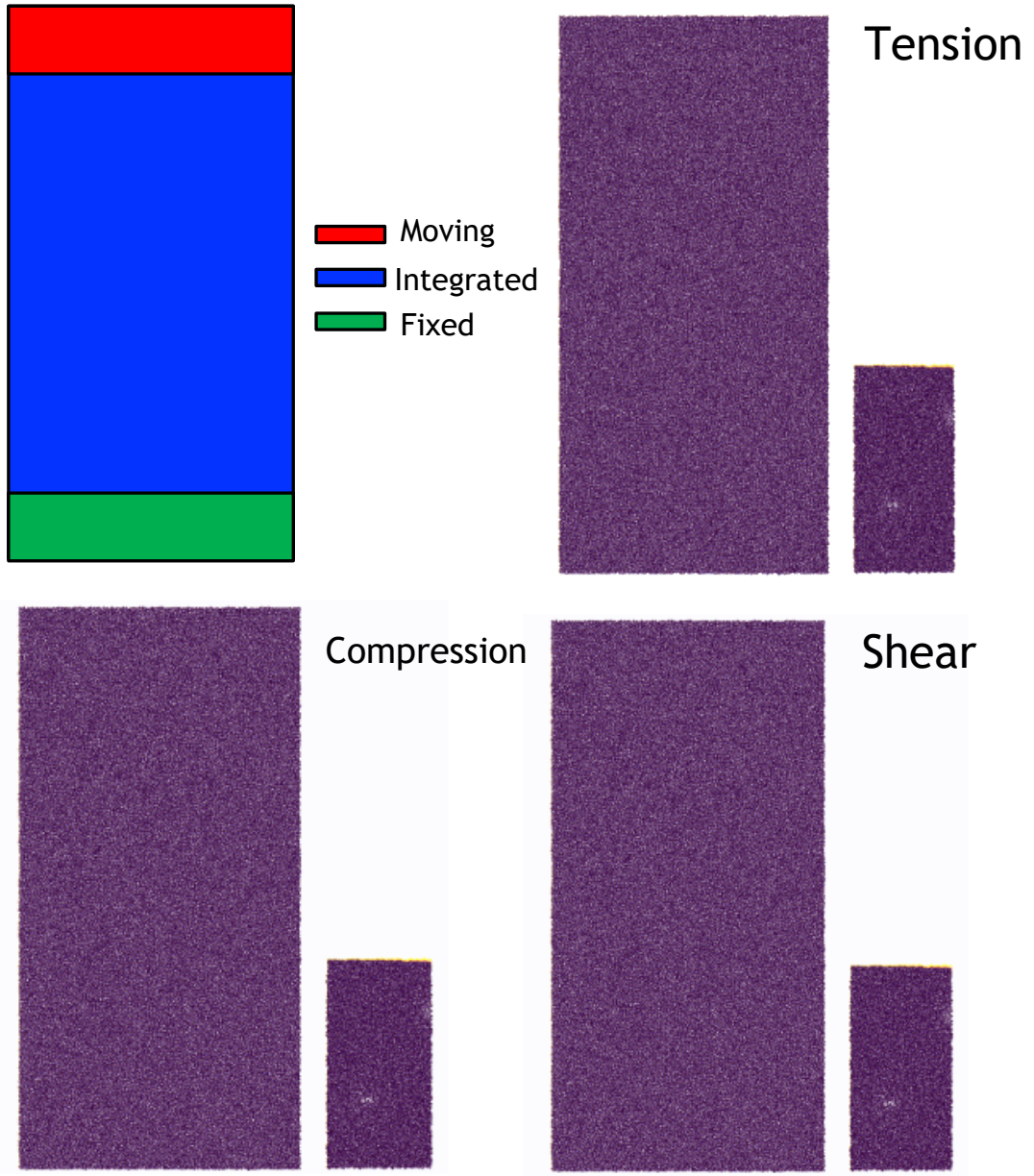

SENSITIVITY ANALYSIS RESULTS

- Sobol sensitivity examines how input parameters affect variance of expected value.
- Total sensitivity
  - Includes all parameter interactions.
  - Similar trends for all three cases.
  - Poisson ratio has the largest impact.
- First order sensitivity
  - Direct effect of given parameter on variance of expected value.
  - Excludes higher-order interactions between parameters.
  - Differences in parameter importance between the test cases.
  - Compression: Elastic modulus and friction angle.
  - Shear: Elastic modulus and plastic friction coefficient.
  - Tension: Plastic friction coefficient and plastic hardening coefficient.

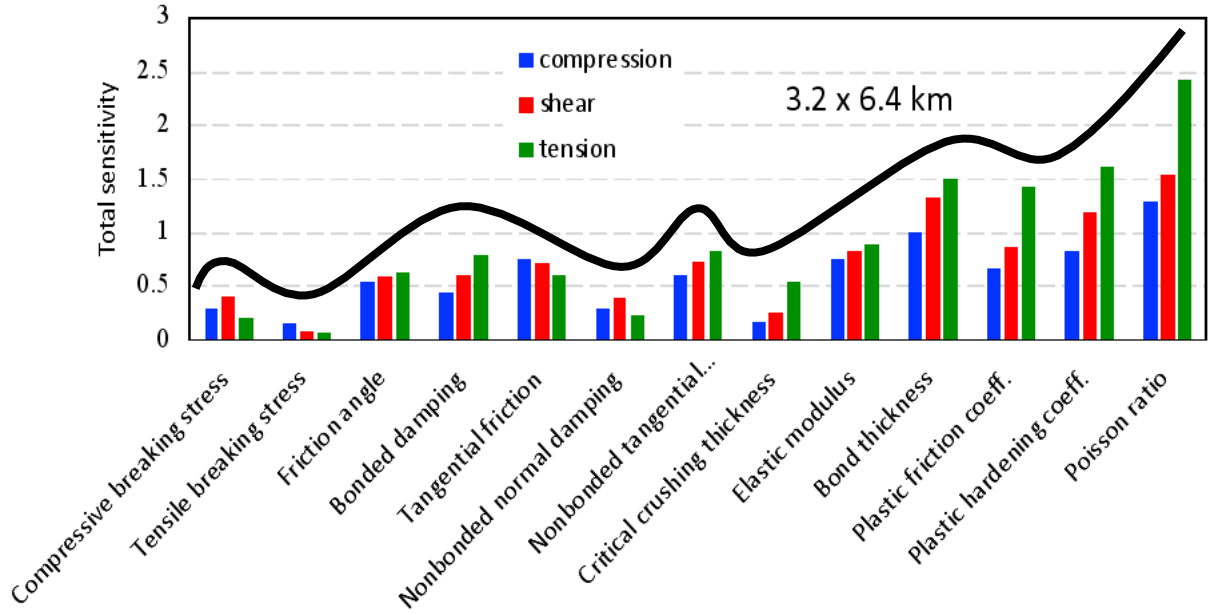

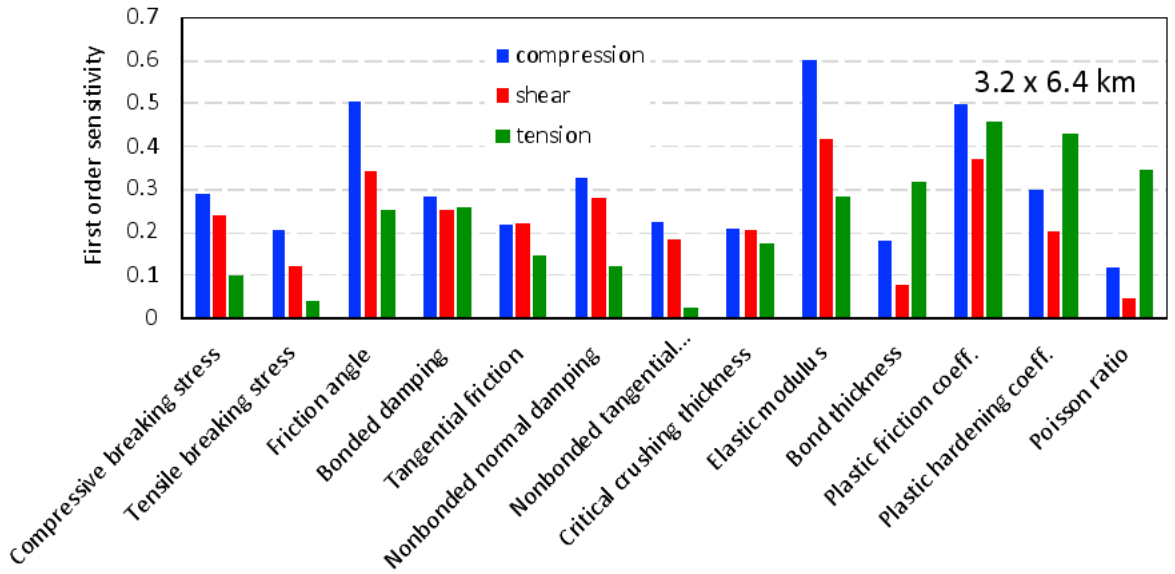

SENSITIVITY ANALYSIS SIZE IMPA

- No size dependence in compression.
- Plastic friction coefficient shows size dependence in shear.
- In tension total sensitivities shows strong size dependence.
  - Possibly due to local heterogeneity in 1.2 x 2.4 km sample.

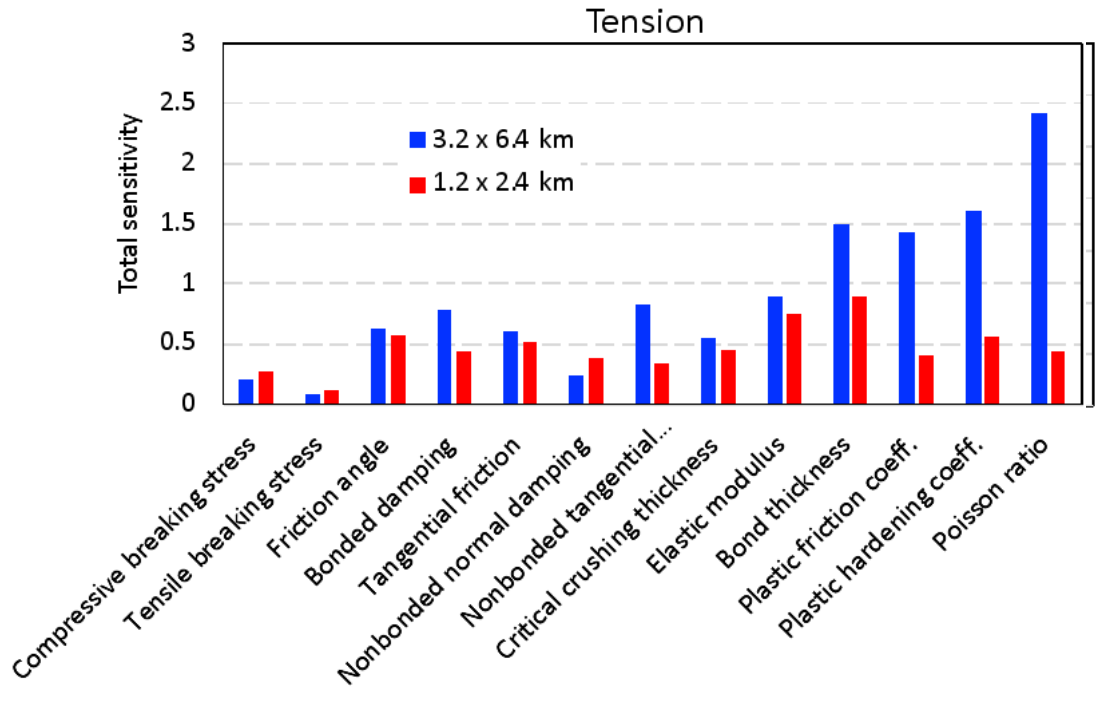

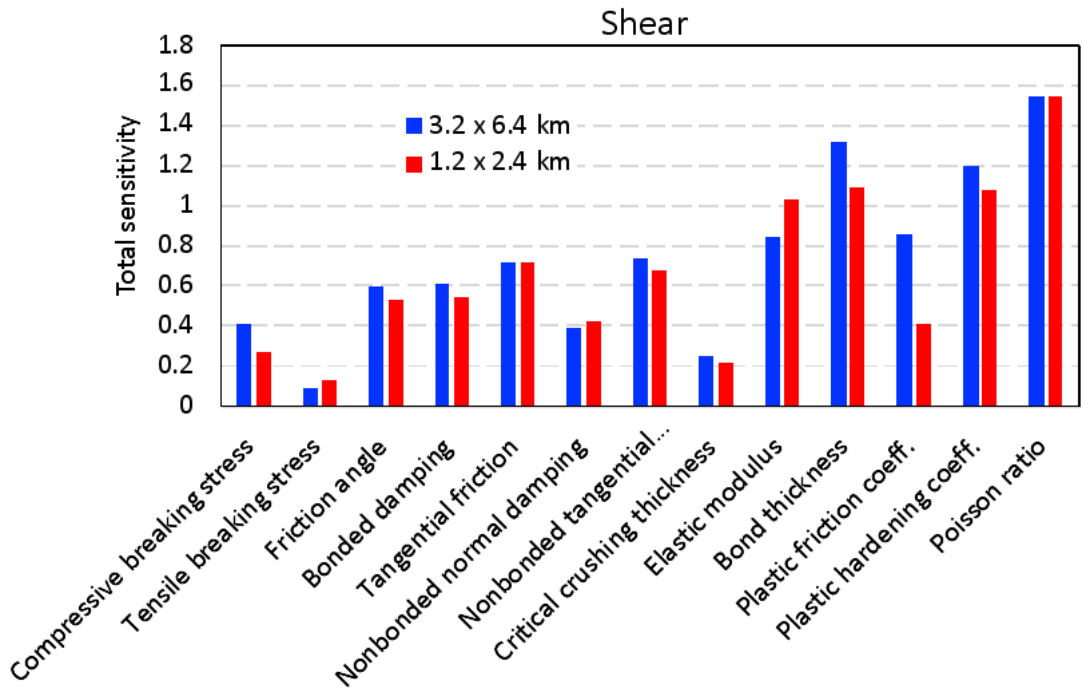

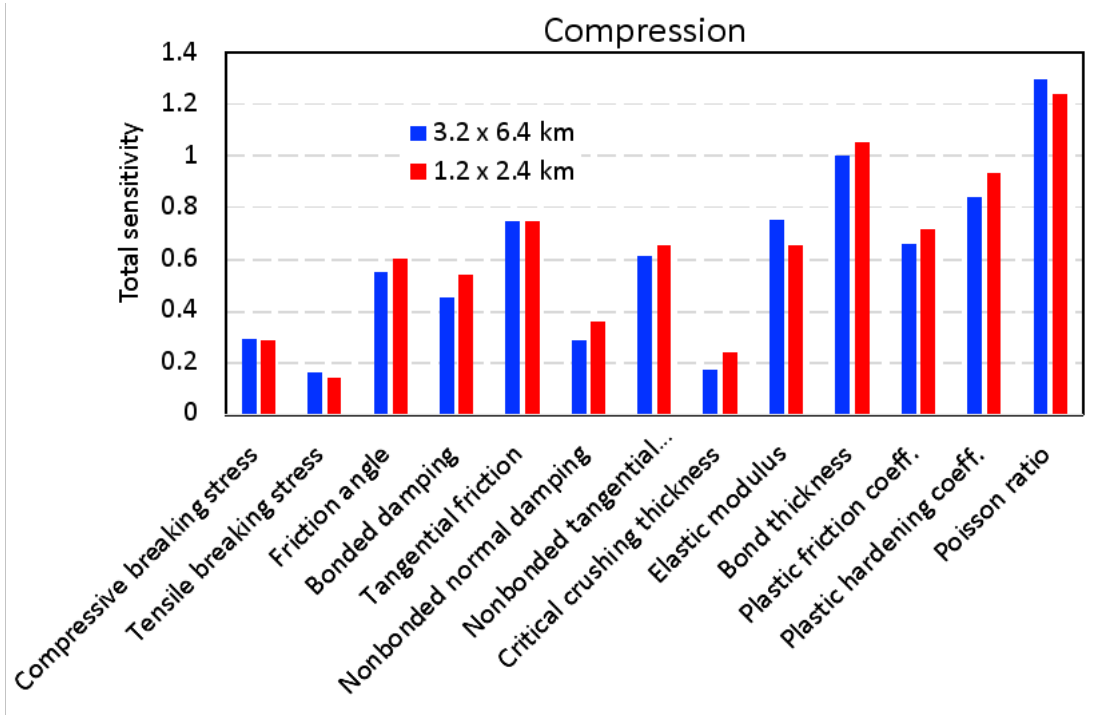

PARAMETER SENSITIVITY FOR MORE COMPLEX GEOMETRIES

- Delta & Sobol sensitivity analyses conducted.
- Using 3584 samples drawn from Saltelli distribution.
- Delta sensitivity analysis examines relation between PDF of input/output values.

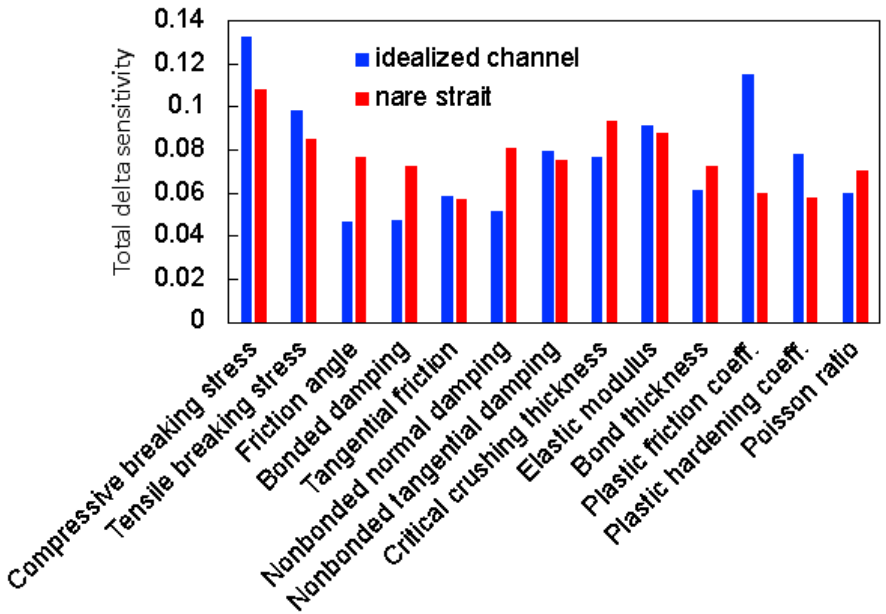

Idealized Channel

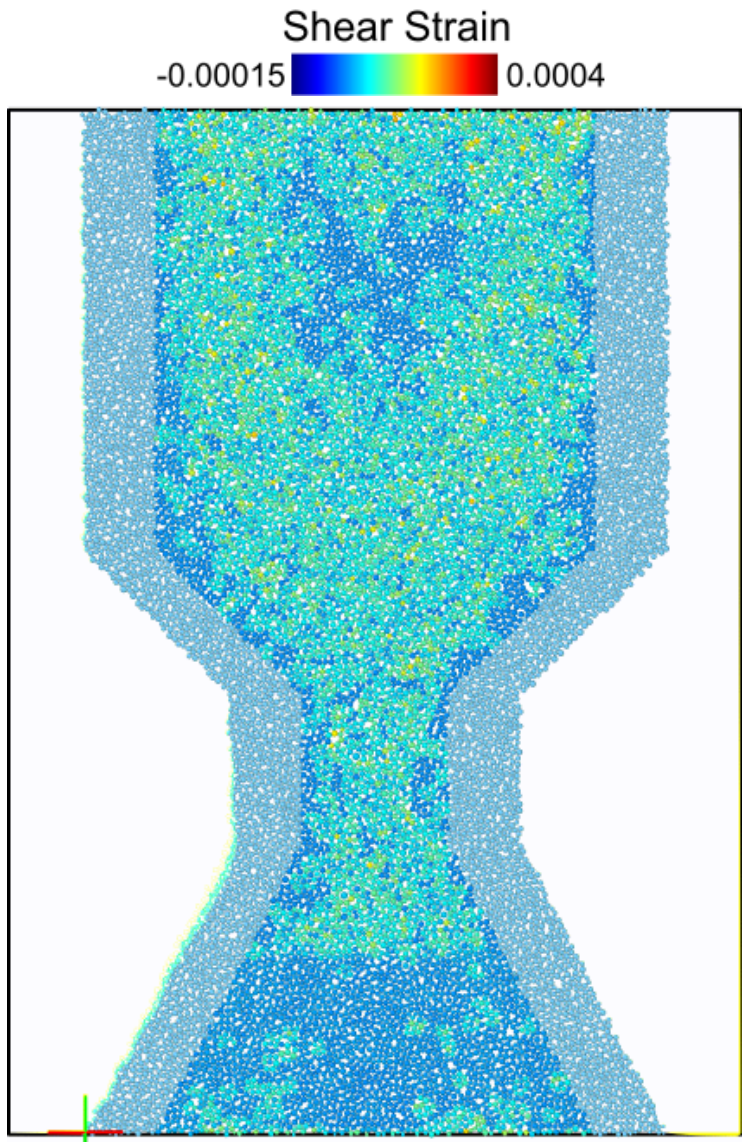

Nares Strait: Kane Basin Volumetric Strain

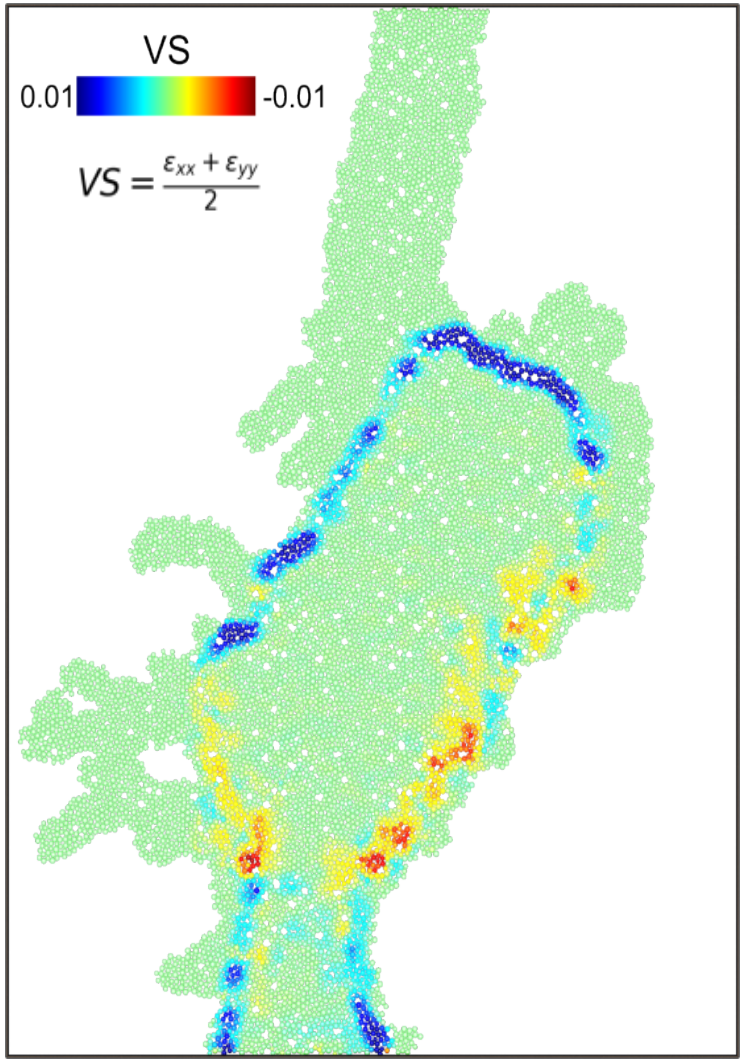

CONCLUSIONS

DEMSI under development as a component of Energy Exascale Earth System Model (E3SM)

- Leverages LAMMPS and IcePack libraries.
- Incorporates bonded and unbonded contact model.
- Implements conservative particle remap algorithm to handle new ice growth and particle clustering.

- Contact model parameter sensitivity analysis performed
  - Identified important parameters.
  - Next steps are parameter calibration and optimization.

Northern hemisphere sea ice concentration
Average element radius is ~20km

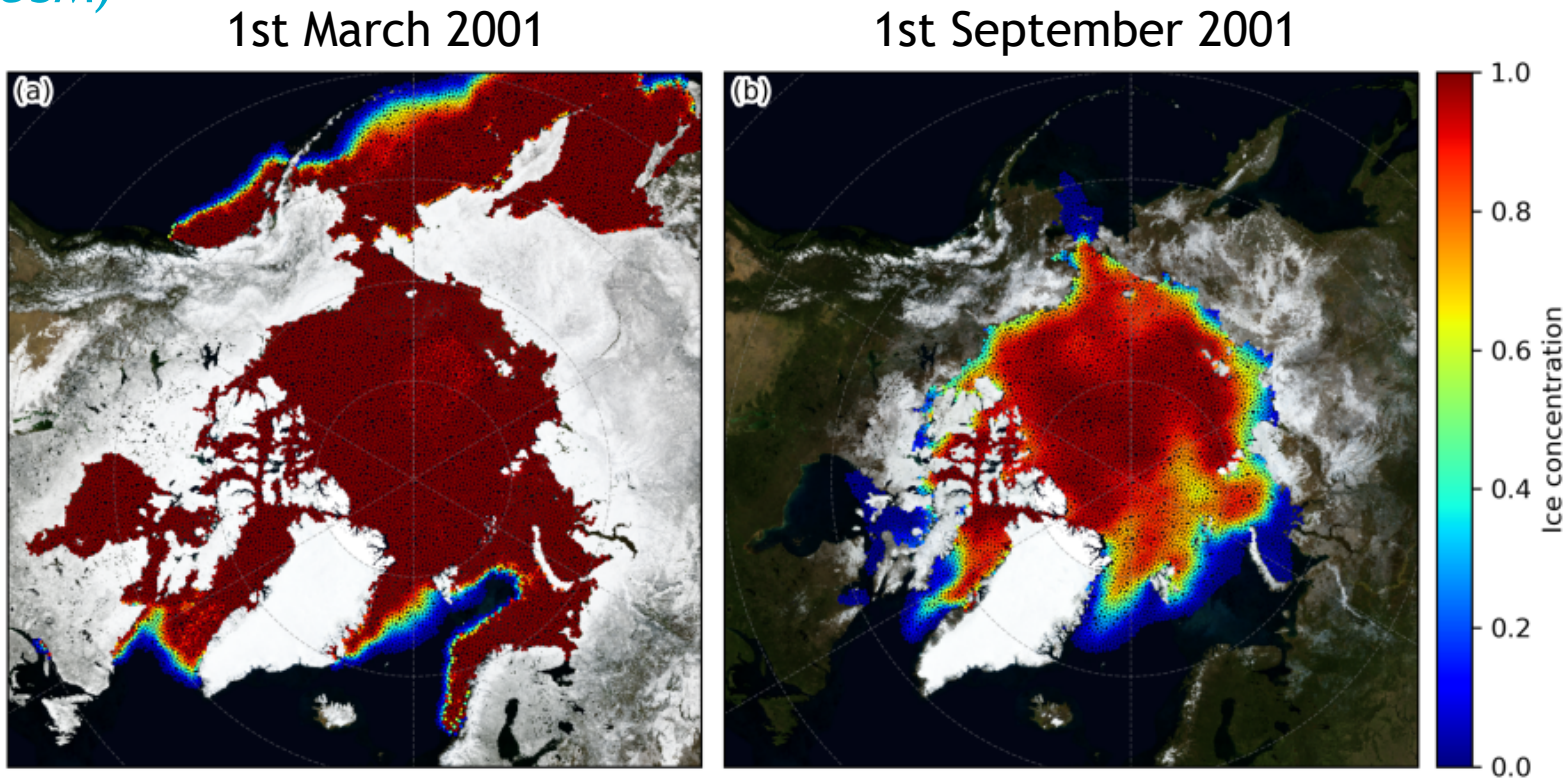

REFERENCES

- Herman, A., Discrete-Element bonded-particle Sea Ice model DESIgn, version 1.3a – model description and implementation, *GMD*, 9, 1219–1241, https://doi:10.5194/gmd-9-1219-2016 , 2016.
- Hopkins, M. A., A discrete element Lagrangian sea ice model, Engineering Computations, 21, 2–4, 2004.
- Hunke, E., R. Allard, D. Bailey, P. Blain, T. Craig, A. Damsgaard, F. Dupont, A. DuVivier, R. Grumbine, M. Holland, N. Jeffery, J.-F. Lemieux, A. Roberts, M. Turner, and M. Winton, CICE consortium/icepack version 1.1.0 (version icepack1.1.0), *Zenodo*, https://doi:10.5281/zenodo.1891650 2018.
- Rampal, P., Bouillon, S., Ólason, E., and Morlighem, M.: neXtSIM: a new Lagrangian sea ice model, The Cryosphere, 10, 1055–1073, https://doi.org/10.5194/tc-10-1055-2016 , 2016.
- Thompson, A. P., H. M. Aktulga, R. Berger, D. S. Bolintineanu, W. M. Brown, P. S. Crozier, P. J. in 't Veld, A. Kohlmeyer, S. G. Moore, T. D. Nguyen, R. Shan, M. J. Stevens, J. Tranchida, C. Trott, S. J. Plimpton, LAMMPS - a flexible simulation tool for particle-based materials modeling at the atomic, meso, and continuum scales,, Comp Phys Comm, 271, 2022.
- Turner, A., K. Peterson, and D. Bolintineanu, Geometric remapping of particle distributions in the Discrete Element Model for Sea Ice. *GMD*, 15, 1953-1970, https://doi.org/10.5194/gmd-15-1953-2022, 2022.
- Turner, A. K., W. H Lipscomb, E. C. Hunke, D. W. Jacobsen, N. Jeffery, D. Engwirda, T. D. Ringler, J. D. Wolfe, MPAS-Seaice (v1.0.0): Sea-ice dynamics on unstructured Voronoi Meshes, *GMD*, 15, 3721–3751, https://doi.org/10.5194/gmd-15-3721-2022, 2022.